

Rounded Layering Transitions on the Surface of Ice

Pablo Llombart^{1,2}, Eva G. Noya^{1,2}, David N. Sibley^{1,3}, Andrew J. Archer^{1,3}, and Luis G. MacDowell^{1,*}

¹*Departamento de Química-Física (Unidad de I+D+i Asociada al CSIC), Facultad de Ciencias Químicas, Universidad Complutense de Madrid, 28040 Madrid, Spain*

²*Instituto de Química Física Rocasolano, CSIC, Calle Serrano 119, 28006 Madrid, Spain*

³*Department of Mathematical Sciences, Loughborough University, Loughborough LE11 3TU, United Kingdom*

 (Received 21 August 2019; revised manuscript received 29 November 2019; accepted 14 January 2020; published 11 February 2020)

Understanding the wetting properties of premelting films requires knowledge of the film's equation of state, which is not usually available. Here we calculate the disjoining pressure curve of premelting films and perform a detailed thermodynamic characterization of premelting behavior on ice. Analysis of the density profiles reveals the signature of weak layering phenomena, from one to two and from two to three water molecular layers. However, disjoining pressure curves, which closely follow expectations from a renormalized mean field liquid state theory, show that there are no layering phase transitions in the thermodynamic sense along the sublimation line. Instead, we find that transitions at mean field level are rounded due to capillary wave fluctuations. We see signatures that true first order layering transitions could arise at low temperatures, for pressures between the metastable line of water-vapor coexistence and the sublimation line. The extrapolation of the disjoining pressure curve above water-vapor saturation displays a true first order phase transition from a thin to a thick film consistent with experimental observations.

DOI: [10.1103/PhysRevLett.124.065702](https://doi.org/10.1103/PhysRevLett.124.065702)

Understanding the properties of the surface of ice is of crucial importance in many important phenomena, such as the growth of snowflakes [1], the freezing and melting rates of ice at the poles [2], or the scavenging of trace gases on ice particles [3]. Interestingly, close to the triple point the ice surface is known to exhibit surface premelting, i.e., the appearance of a loosely defined quasiliquid layer [4], which is expected to have an important effect on crystal growth rates [5], adsorption [3], friction [6], and many other properties [7,8].

But despite its significance, and great experimental progress [4,9–15], the characterization of ice premelting has remained a long-standing matter of debate [7,16,17]. As the controversy regarding the film thickness could start to clarify with agreement between widely different experimental techniques [11,12,18–20], new and exciting observations have been made regarding the properties of the premelting film, both at [15,21,22] and off ice-vapor coexistence [13]. Sanchez *et al.* performed a sum frequency generation experiment (SFG) of the ice surface along the sublimation line and found evidence of a discrete bilayer melting transition [15,17]. Off coexistence, experiments [13] have found a discontinuous transition from a thin to a thick premelting film occurring at water-vapor supersaturation that is often known as frustrated complete wetting [23–26]. An appealing interpretation is to view both phenomena as manifestations of layering effects and renormalization similar to those studied in past decades for simple model systems [27–35]. However, the evidence for

layering is not without some controversy, as other studies also based on SFG suggest that bilayer melting occurs instead in a continuous fashion [14]. Interestingly, computer simulations show that the ice surface exhibits patches of premelted ice, whose size increases continuously as the temperature is increased, also consistent with a continuous buildup of the premelting film [21,22,36].

Here we show that in the range between 230 and 270 K, the order parameter distributions of the main facets of ice exhibit the signature of two consecutive rounded layering transitions. This reconciles conflicting experimental and computer simulation studies of the equilibrium surface structure [14,15,21,22,36]. Extrapolation of our results for the TIP4P/Ice model according to predictions of liquid state and renormalization theory indicates that a genuine first order phase transition occurs at supersaturation, consistent with experimental observations off coexistence [13]. Our results provide a unified vision of the wetting behavior of premelting films on ice.

We use the TIP4P/Ice model, which exhibits a melting temperature of 272 K [37]. To prepare the system in the solid-vapor coexistence region, we place an ice slab of either 1280 or 5120 molecules in vacuum. Performing canonical molecular dynamics simulations [38] with GROMACS, the system attains phase coexistence in a few nanoseconds and an equilibrated premelting film is formed spontaneously [18,39–41] (see Supplemental Material [42]). Previously, computer simulation evidence for a layering transition of the TIP4P/Ice model was discussed

in terms of the density profile $\rho(z)$ of the H_2O molecules as a function of the perpendicular distance z to the interface [15]. A more detailed description of layering phenomena in terms of density profiles is afforded by identifying liquidlike and solidlike environments [43,44]. Using the \bar{q}_6 order parameter [43] allows us to plot the density of liquidlike and solidlike molecules and identify features that are specific to the premelting layer [39,41,45].

The density profile of liquidlike molecules at the {0001} face (or basal face) can be seen in Fig. 1(a). At low temperatures, the profile is highly structured, with the main peaks separated by about 3.5 \AA , a value very close to the preferred lattice spacing of the underlying solid. This, together with the bilayer structure apparent as a double peak, is suggestive of a rather ordered liquidlike environment. As temperature rises, the profiles transform in a continuous manner up to about 267 K. At this temperature a qualitative change is observed, as the outermost maxima and minima of the density profile disappear via an inflection point, leaving the profile with a monotonic decay into the vapor phase.

In fact, the strong stratification of the liquidlike profile is caused to a great extent by the structure of the underlying ice lattice. To show this, we describe the premelting liquid layer in terms of two bounding surfaces separating the quasiliquid (fluid) film from bulk ice and bulk vapor [39,41,45]. For points \mathbf{x} along a flat reference plane, we calculate an ice-film (i - f) surface as the loci $z_{i-f}(\mathbf{x})$ of the outermost solidlike molecules. Likewise, we calculate a film-vapor (f - v) surface as the loci $z_{f-v}(\mathbf{x})$ of the outermost liquidlike molecules (see Supplemental Material [42]). An intrinsic density profile relative to the local f - v interface can then be determined as the density of atoms at a distance $z - z_{f-v}(\mathbf{x})$. The picture that emerges [Fig. 1(b)] shows a much less layered structure, confirming that the strong stratification of $\rho(z)$ shown in Fig. 1(a) is largely the result of structural correlations conveyed by the solid phase. The profile evolves continuously up to 264 K, with the outermost minimum and maximum

again disappearing across an inflection point at about $z - z_{f-v}(\mathbf{x}) = -2.2 \text{ \AA}$, as the decay of the density profile toward the vapor phase takes the monotonic form characteristic of a liquid-vapor interface.

The same insight can be found by plotting the intrinsic density profile of liquidlike molecules as measured relative to the fluctuating i - f surface [Fig. 1(c)], which is again less stratified than the absolute density profile. This profile also evolves in a rather continuous fashion, but, surprisingly, it does not show any particular signature of layering between 265 and 270 K as observed previously. Rather, in this case one notices the appearance of a maximum at about 6.7 \AA , which occurs via an inflection point between 230 and 235 K.

While the details of the liquidlike density profiles at the prism facet {10 $\bar{1}$ 0} are very different, the main features observed at the basal facet are also found here, with intrinsic density profiles that are again very much rounded relative to the strongly stratified absolute density profile. A close inspection shows inflection points appear between 265 and 270 K and between 240 and 250 K (see Supplemental Material [42]).

In order to clarify the process of bilayer melting further, we need to resort to a more illuminating order parameter than the density profiles of liquidlike molecules. Based on the intrinsic i - f and f - v surfaces, we can define an instantaneous local film thickness as $\hat{h}(\mathbf{x}) = z_{f-v}(\mathbf{x}) - z_{i-f}(\mathbf{x})$. We exploit this local parameter to calculate the mean film thickness h after lateral and canonical averaging over the simulation run.

Figure 2(a) depicts the results obtained for the basal plane. The film thickness grows from about one molecular layer at $T = 210 \text{ K}$ to about three molecular layers at $T = 270 \text{ K}$ in a continuous fashion, with no clear evidence of a first order layering transition. Results obtained recently for the Monoatomic Water model (mW) show a similar trend but appear smoother as they are sampled in the grand canonical ensemble, which allows for larger film thickness fluctuations [21,22]. We provide a full thermodynamic

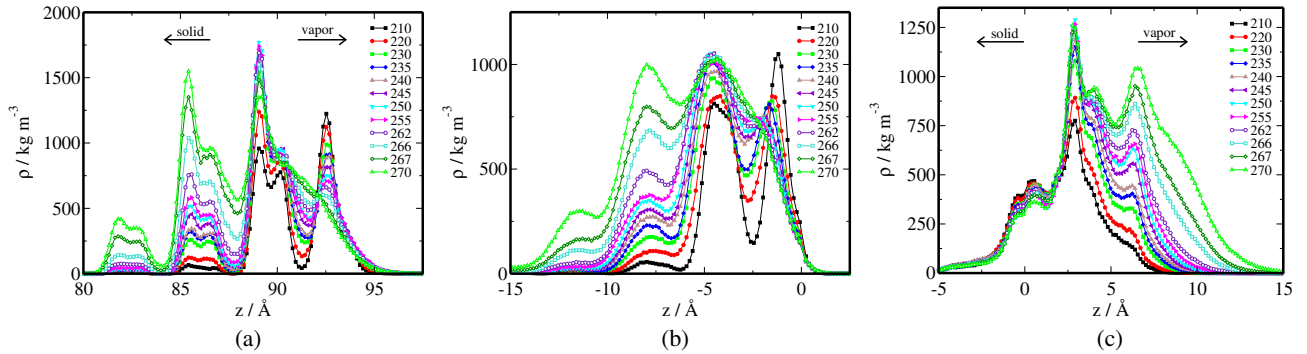


FIG. 1. Density profiles of liquidlike molecules for the basal interface as measured relative to (a) the laboratory reference frame, (b) the f - v surface, and (c) the i - f surface. Since the liquidlike layer has finite thickness, the profiles vanish at the solid phase to the left and the vapor phase to the right of the z axis.

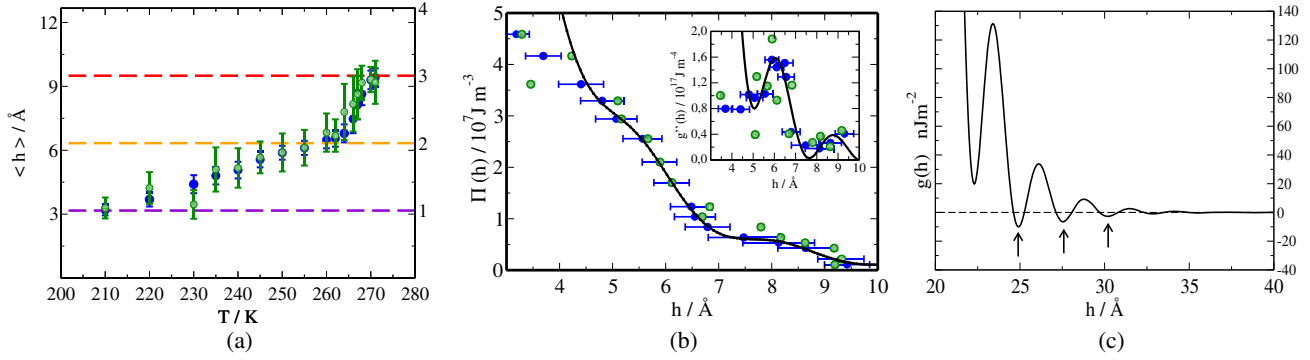


FIG. 2. Film thickness (a), disjoining pressure (b), and interface potential (c) for the basal facet. Results are shown for two system sizes with $n_x \times n_y = 5120$ (blue filled circles) and $n_x \times n_y = 1280$ (green hollow circles) molecules. (a) The dashed lines indicate discrete film heights in units of the molecular diameter. (b) The lines are a fit to Eq. (2) to the blue symbols for $h > 4.0 \text{ \AA}$. The insets show inverse surface susceptibilities as obtained from numerical derivatives (symbols) and from analytical derivatives of the fits (lines). Error bars are shown here only for the system fitted to Eq. (2). Panel (c) shows the decay of the interface potential at intermediate distances as extrapolated from the fit to Eq. (2). Arrows indicate states that can transition at supersaturation, i.e., to frustrated complete wetting states.

characterization of wetting properties by calculating the disjoining pressure of the film, $\Pi(h) = -dg(h)/dh$, where $g(h)$ is the binding potential, which accounts for the pressure difference between the adsorbed liquid film and the bulk vapor of equal chemical potential, i.e., [46–48]

$$\Pi(h) = p_v(\mu, T) - p_l(\mu, T). \quad (1)$$

In practice, $\Pi(h)$ is to an adsorbed liquid film as the Laplace pressure is to a liquid droplet. In particular, the vapor pressure of an ideal gas in equilibrium with a film of thickness h is given in a manner analogous to the Kelvin-Laplace equation as $p_v = p_{v,w} e^{-\beta\Pi(h)/\rho_w}$, where $p_{v,w}$ is the saturated vapor pressure over water, ρ_w is the bulk liquid density at coexistence, and $\beta = (k_B T)^{-1}$. An equilibrium film thickness for water adsorbed at the ice-vapor interface can be meaningfully defined only along the sublimation line, where the vapor pressure equals the saturated vapor pressure over ice $p_{v,i}$. Accordingly, the above equation becomes $p_{v,i} = p_{v,w} e^{-\beta\Pi(h)/\rho_w}$. It follows that using accurate coexistence vapor pressures, and the corresponding equilibrium film thickness $h(T)$ along the sublimation line, we can readily determine $\Pi(h)$ (Supplemental Material [42]). The significance of this result can hardly be overemphasized. By exploiting the data $h(T)$ at solid-vapor coexistence, we can now determine the film height of the premelting film at arbitrary temperature and pressure, by merely solving Eq. (1) for h [49]. This is a required input in theories of premelting [5,50,51].

Results for the basal surface are shown in Fig. 2(b). The disjoining pressure curve measured up to $h = 10 \text{ \AA}$ exhibits a monotonic behavior, but with a clear damped oscillatory decay at positive disjoining pressure. In contrast, a system exhibiting first order layering transitions exhibits sinusoidal oscillations in mean field, or alternatively, an equal areas Maxwell construction with a segment of zero

slope beyond mean field. We confirm the presence of the oscillatory behavior from plots of the derivative (obtained numerically)—see inset. Maxima of the inverse susceptibility, $\chi_{\parallel}^{-1} = d^2g/dh^2$, which characterizes parallel correlations, indicate enhanced stability at preferred film thicknesses of $h = 6 \text{ \AA}$ for the basal plane and at $h = 5.4 \text{ \AA}$ for the prism plane (Supplemental Material [42]), but this is not a sufficient criteria for a thermodynamic phase transition. Thus, it appears that at a mean field level there could be layering which is washed away upon renormalization to larger length scales, as suggested from the study of capillary wave fluctuations [30,33].

Liquid state theory provides an expansion for the renormalized interface potential $g(h)$ of a premelting film dominated by short-range structural forces. To leading order in h , this gives

$$g_R(h) = A_2 e^{-\kappa h} - A_1 e^{-\kappa_R h} \cos(k_{z,R} h), \quad (2)$$

where the amplitudes A_1 and A_2 depend on T , while κ and κ_R are inverse length scales that characterize the decay of the pair correlations in the liquid. Their values are renormalized from those one would expect on the basis of mean field theory, so that, e.g., $k_{z,R} < k_z$, where k_z is the wave number corresponding to the maximum of the bulk liquid structure factor [30,32,33,52,53].

This result is an asymptotic form, and is not expected to hold for small thicknesses of barely one molecular diameter. However, a fit of $\Pi(h) = -dg_R(h)/dh$ as predicted by Eq. (2) for all $h > 4.0 \text{ \AA}$ exhibits an excellent agreement with simulation data. Moreover, from the fitting parameters we can determine the wetting behavior at short and intermediate h . For the basal facet ($\kappa = 0.61 \text{ \AA}^{-1}$, $\kappa_R = 0.43 \text{ \AA}^{-1}$, and $k_{z,R} = 2.36 \text{ \AA}^{-1}$), we find $\kappa_R < \kappa$, so that $g(h)$ exhibits an absolute minima at intermediate distances.

This implies incomplete wetting of the premelting film, as expected for facets below the roughening temperature of the solid-melt interface [30,32,33]. For the prism plane ($\kappa = 0.62 \text{ \AA}^{-1}$, $\kappa_R = 0.90 \text{ \AA}^{-1}$, and $k_{z,R} = 3.14 \text{ \AA}^{-1}$), we find in contrast that $\kappa_R > \kappa$, so that $g(h)$ exhibits a monotonic decay. This leads to complete wetting of the premelting film as a result of a fluctuation dominated wetting transition [30]. Of course, for very large h the decay rate of κ_R is not expected to depend on the crystal facet. However, for intermediate values of h of interest here, the decay need not be exactly the same, since the renormalized quantities depend on details of the interface potential at short range. In practice, at sufficiently large distance, van der Waals forces with algebraic decay will favor incomplete wetting irrespective of the surface plane involved [54].

To clarify whether the layering is consistent with either a continuous or a first order phase transition, we perform a block analysis of the film thickness distributions [55,56] and plot the probability distribution of film thicknesses averaged over lateral areas of increasing size. We consider $h(\mathbf{x})$, which accounts for a lateral size of two unit cells; $h_{1/4}$, which accounts for an average over a quarter of the full system; and h , an average over the full system size. The results are presented in Fig. 3.

For the local order parameter $h(\mathbf{x})$, we find rather broad distributions, which span as much as 9 \AA , i.e., ≈ 3 molecular diameters. In the event of a first order phase transition, broad distributions found in small systems become bimodal, with two sharp peaks separated by a gap of increasingly smaller probability as the system size grows. Contrary to this scenario, the block analysis performed over distributions of $h_{1/4}$ and h shows that no signs of bimodality persist in any of these distributions, the peaks appear to sharpen significantly, and the gap between two and three layers is filled with unimodal distributions. However, the distributions corresponding to fully formed layers are clearly much sharper, while those corresponding

to distances in between remain broader, i.e., exhibit enhanced fluctuations. This scenario resembles that of a continuous phase transition in a finite system [55,56], but our block analysis does not show evidence of singular behavior. Accordingly, it appears that the system is traversing the prolongation of a first order phase transition beyond the critical point, across a continuous and nonsingular transition. This explains why SFG experiments, which probe a local order parameter, can detect distinct spectral changes of the local environment as temperature is raised.

Indeed, an analysis of average mean square fluctuations and higher moments (Supplemental Material [42]) reveals the signature of two rounded layering transitions on the basal plane, first, from one to two bilayers, at about $T = 235 \text{ K}$, then from two to three bilayers at $T = 267 \text{ K}$. These transitions very much correlate with the inflection points observed previously in the density profiles. The latter is consistent with results by Sanchez *et al.* for the TIP4P/Ice model, which bracketed the bilayer melting between 260 and 270 K [15]. Hints of an inflection in the premelting film thickness that could be consistent with the same phenomena are also observable in the mW model at about 260 K [21,22]. For the primary prism plane (Supplemental Material [42]) the results are similar and reveal the presence of two rounded transitions at about 250 and 267 K, as suggested from the study of inflection points in the density profile. The transitions at 235 and 250 K observed for basal and prism planes correlate with the onset of surface mobility reported recently for the same model [40].

Interestingly, the distance between maxima of the global order parameter distribution increases with film height. For the basal plane the three maxima are separated by 2.9 and 3.4 \AA , respectively. For the prism plane, the separation is 2.3, 2.7, and 3.6 \AA , respectively. This is again consistent with the renormalization scenario, since we expect the renormalization of k_z to be more significant as the distance from the substrate increases. Thus, it might be possible that

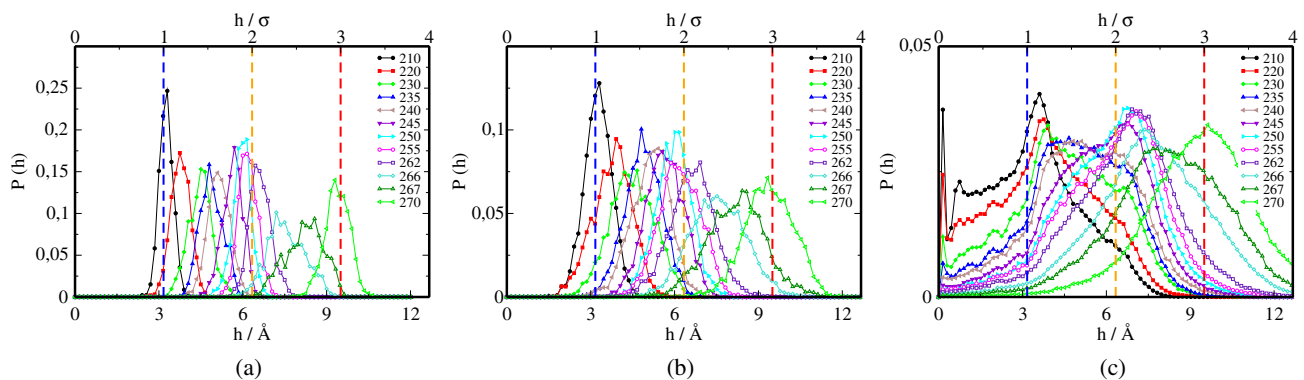


FIG. 3. System size analysis of thickness distributions at the basal plane. (a) Probability distribution of the global film thickness h . (b) Probability distribution of the partial film thickness $h_{1/4}$. (c) Probability distribution of the local order parameter $h(\mathbf{x})$. Dashed vertical lines show the film thickness in units of the molecular diameter. Results are shown for temperatures in the range from $T = 210 \text{ K}$ to $T = 271 \text{ K}$, with color code as indicated in each panel.

true first order transitions occur for large h between adjacent minima that are several molecular diameters apart as a result of renormalization. This view provides an explanation for the experimental observation of frustrated complete wetting in confocal microscopy experiments [13].

In summary, we document the existence of rounded layering transitions with enhanced fluctuations at 235 and 267 K for the basal interface and at 250 and 267 K for the prism interface. We conjecture that the continuation of a line of true first order layering transitions beyond the layering critical point could intersect the sublimation line and explain the enhanced fluctuations observed here. This reconciles conflicting interpretations of layering on the ice surface [14,15,22] and opens exciting new avenues for experimental verification.

We would like to acknowledge Enrique Lomba for helpful discussions and Jose Luis F. Abascal for support. We acknowledge use of the MareNostrum supercomputer and the technical support provided by Barcelona Supercomputing Center from Red Española de Supercomputación (RES) under Grants No. QCM-2017-2-0008 and No. QCM-2017-3-0034. We also acknowledge funding from the Spanish Agencia Estatal de Investigación (AEI) and the Fondo Europeo de Desarrollo Regional (FEDER) under Grant No. FIS2017-89361-C3-2-P(AEI/FEDER,UE).

*lgmac@quim.ucm.es

- [1] K. G. Libbrecht, Physical dynamics of ice crystal growth, *Annu. Rev. Mater. Res.* **47**, 271 (2017).
- [2] J. G. Dash, A. W. Rempel, and J. S. Wettlaufer, The physics of premelted ice and its geophysical consequences, *Rev. Mod. Phys.* **78**, 695 (2006).
- [3] J. P. D. Abbatt, Interactions of atmospheric trace gases with ice surfaces: Adsorption and reaction, *Chem. Rev.* **103**, 4783 (2003).
- [4] Y. Furukawa, M. Yamamoto, and T. Kuroda, Ellipsometric study of the transition layer on the surface of an ice crystal, *J. Cryst. Growth* **82**, 665 (1987).
- [5] T. Kuroda and R. Lacmann, Growth kinetics of ice from the vapour phase and its growth forms, *J. Cryst. Growth* **56**, 189 (1982).
- [6] B. Weber, Y. Nagata, S. Ketzetzi, F. Tang, W. J. Smit, H. J. Bakker, E. H. G. Backus, M. Bonn, and D. Bonn, Molecular insight into the slipperiness of ice, *J. Phys. Chem. Lett.* **9**, 2838 (2018).
- [7] B. Slater and A. Michaelides, Surface premelting of water ice, *Nat. Rev. Chem.* **3**, 172 (2019).
- [8] Y. Nagata, T. Hama, E. H. G. Backus, M. Mezger, D. Bonn, M. Bonn, and G. Sazaki, The surface of ice under equilibrium and nonequilibrium conditions, *Acc. Chem. Res.* **52**, 1006 (2019).
- [9] H. Dosch, A. Lied, and J. H. Bilgram, Disruption of the hydrogen-bonding network at the surface of I_h ice near surface premelting, *Surf. Sci.* **366**, 43 (1996).
- [10] X. Wei, P. B. Miranda, and Y. R. Shen, Surface Vibrational Spectroscopic Study of Surface Melting of Ice, *Phys. Rev. Lett.* **86**, 1554 (2001).
- [11] H. Bluhm, D. F. Ogletree, C. S. Fadley, Z. Hussain, and M. Salmeron, The premelting of ice studied with photoelectron spectroscopy, *J. Phys. Condens. Matter* **14**, L227 (2002).
- [12] V. Sadtschenko and G. E. Ewing, Interfacial melting of thin ice films: An infrared study, *J. Chem. Phys.* **116**, 4686 (2002).
- [13] K.-I. Murata, H. Asakawa, K. Nagashima, Y. Furukawa, and G. Sazaki, Thermodynamic origin of surface melting on ice crystals, *Proc. Natl. Acad. Sci. U.S.A.* **113**, E6741 (2016).
- [14] W. J. Smit and H. J. Bakker, The surface of ice is like supercooled liquid water, *Angew. Chem., Int. Ed. Engl.* **56**, 15540 (2017).
- [15] M. A. Sánchez, T. Kling, T. Ishiyama, M.-J. van Zadel, P. J. Bisson, M. Mezger, M. N. Jochum, J. D. Cyran, W. J. Smit, H. J. Bakker, M. J. Shultz, A. Morita, D. Donadio, Y. Nagata, M. Bonn, and E. H. G. Backus, Experimental and theoretical evidence for bilayer-by-bilayer surface melting of crystalline ice, *Proc. Natl. Acad. Sci. U.S.A.* **114**, 227 (2017).
- [16] Y. Li and G. A. Somorjai, Surface premelting of ice, *J. Phys. Chem. C* **111**, 9631 (2007).
- [17] A. Michaelides and B. Slater, Melting the ice one layer at a time, *Proc. Natl. Acad. Sci. U.S.A.* **114**, 195 (2017).
- [18] M. M. Conde, C. Vega, and A. Patrykiewicz, The thickness of a liquid layer on the free surface of ice as obtained from computer simulation, *J. Chem. Phys.* **129**, 014702 (2008).
- [19] J. Gelman Constantin, M. M. Gianetti, M. P. Longinotti, and H. R. Corti, The quasi-liquid layer of ice revisited: the role of temperature gradients and tip chemistry in AFM studies, *Atmos. Chem. Phys.* **18**, 14965 (2018).
- [20] T. Mitsui and K. Aoki, Fluctuation spectroscopy of surface melting of ice with and without impurities, *Phys. Rev. E* **99**, 010801(R) (2019).
- [21] I. Pickering, M. Paleico, Y. A. P. Sirkin, D. A. Scherlis, and M. H. Factorovich, Grand canonical investigation of the quasi liquid layer of ice: Is it liquid?, *J. Phys. Chem. B* **122**, 4880 (2018).
- [22] Y. Qiu and V. Molinero, Why is it so difficult to identify the onset of ice premelting, *J. Phys. Chem. Lett.* **9**, 5179 (2018).
- [23] N. Shahidzadeh, D. Bonn, K. Ragil, D. Broseta, and J. Meunier, Sequence of Two Wetting Transitions Induced by Tuning the Hamaker Constant, *Phys. Rev. Lett.* **80**, 3992 (1998).
- [24] J. O. Indekeu, K. Ragil, D. Bonn, D. Broseta, and J. Meunier, Wetting of alkanes on water from a Cahn-type theory: Effects of long-range forces, *J. Stat. Phys.* **95**, 1009 (1999).
- [25] M. Müller and L. G. MacDowell, Wetting of a short chain fluid on a brush: First order and critical wetting transitions, *Europhys. Lett.* **55**, 221 (2001).
- [26] L. G. MacDowell and M. Müller, Observation of autophobic dewetting on polymer brushes from computer simulation, *J. Phys. Condens. Matter* **17**, S3523 (2005).
- [27] J. D. Weeks, Variational theory of multilayer solid adsorption, *Phys. Rev. B* **26**, 3998 (1982).
- [28] D. A. Huse, Renormalization-group analysis of layering transitions in solid films, *Phys. Rev. B* **30**, 1371 (1984).

- [29] A. Patrykiewicz, D. Landau, and K. Binder, Lattice gas models for multilayer adsorption: variation of phase diagrams with the strength of the substrate potential, *Surf. Sci.* **238**, 317 (1990).
- [30] A. A. Chernov and L. V. Mikheev, Wetting of Solid Surfaces by a structured Simple Liquid: Effect of Fluctuations, *Phys. Rev. Lett.* **60**, 2488 (1988).
- [31] P. C. Ball and R. Evans, Structure and adsorption at gas-solid interfaces: Layering transitions from a continuum theory, *J. Chem. Phys.* **89**, 4412 (1988).
- [32] R. Evans, Density functionals in the theory of nonuniform fluids, in *Fundamentals of Inhomogeneous Fluids*, edited by D. Henderson (Marcel Dekker, New York, 1992), Chap. 3, pp. 85–175.
- [33] J. R. Henderson, Wetting phenomena and the decay of correlations at fluid interfaces, *Phys. Rev. E* **50**, 4836 (1994).
- [34] J. M. Brader, R. Evans, M. Schmidt, and H. Löwen, Entropic wetting and the fluid–fluid interface of a model colloid–polymer mixture, *J. Phys. Condens. Matter* **14**, L1 (2001).
- [35] M. Dijkstra and R. van Roij, Entropic Wetting and Many-Body Induced Layering in a Model Colloid-Polymer Mixture, *Phys. Rev. Lett.* **89**, 208303 (2002).
- [36] A. Hudait, M. T. Allen, and V. Molinero, Sink or swim: Ions and organics at the ice-air interface, *J. Am. Chem. Soc.* **139**, 10095 (2017).
- [37] J. L. F. Abascal, E. Sanz, R. G. Fernandez, and C. Vega, A potential model for the study of ices and amorphous water: TIP4P/Ice, *J. Chem. Phys.* **122**, 234511 (2005).
- [38] G. Bussi, D. Donadio, and M. Parrinello, Canonical sampling through velocity rescaling, *J. Chem. Phys.* **126**, 014101 (2007).
- [39] J. Benet, P. Llombart, E. Sanz, and L. G. MacDowell, Premelting-Induced Smoothing of the Ice-Vapor Interface, *Phys. Rev. Lett.* **117**, 096101 (2016).
- [40] T. Kling, F. Kling, and D. Donadio, Structure and dynamics of the quasi-liquid layer at the surface of ice from molecular simulations, *J. Phys. Chem. C* **122**, 24780 (2018).
- [41] P. Llombart, R. M. Bergua, E. G. Noya, and L. G. MacDowell, Structure and water attachment rates of ice in the atmosphere: Role of nitrogen, *Phys. Chem. Chem. Phys.* **21**, 19594 (2019).
- [42] See Supplemental Material at <http://link.aps.org/supplemental/10.1103/PhysRevLett.124.065702> for results of prism facet, underpinning thermodynamic calculations, fluctuation analysis and simulation details.
- [43] W. Lechner and C. Dellago, Accurate determination of crystal structures based on averaged local bond order parameters, *J. Chem. Phys.* **129**, 114707 (2008).
- [44] A. H. Nguyen and V. Molinero, Identification of clathrate hydrates, hexagonal ice, cubic ice, and liquid water in simulations: the chill+ algorithm, *J. Phys. Chem. B* **119**, 9369 (2015).
- [45] J. Benet, P. Llombart, E. Sanz, and L. G. MacDowell, Structure and fluctuations of the premelted liquid film of ice at the triple point, *Mol. Phys.* **117**, 2846 (2019).
- [46] B. Derjaguin, Modern state of the investigation of long-range surface forces, *Langmuir* **3**, 601 (1987).
- [47] J. R. Henderson, Statistical mechanics of the disjoining pressure of a planar film, *Phys. Rev. E* **72**, 051602 (2005).
- [48] J. Benet, J. G. Palanco, E. Sanz, and L. G. MacDowell, Disjoining pressure, healing distance, and film height dependent surface tension of thin wetting films, *J. Phys. Chem. C* **118**, 22079 (2014).
- [49] D. Sibley, P. Llombart, E. G. Noya, A. Archer, and L. G. MacDowell (to be published).
- [50] D. Nenow and A. Trayanov, Thermodynamics of crystal surfaces with quasi-liquid layer, *J. Cryst. Growth* **79**, 801 (1986).
- [51] J. S. Wettlaufer, Surface phase transitions in ice: From fundamental interactions to applications, *Phil. Trans. R. Soc. A. Math. Phys. Eng. Sci.* **377**, 20180261 (2019).
- [52] R. Evans, R. J. F. L. de Carvalho, J. R. Henderson, and D. C. Hoyle, Asymptotic decay of correlations in liquids and their mixtures, *J. Chem. Phys.* **100**, 591 (1994).
- [53] A. P. Hughes, U. Thiele, and A. J. Archer, Influence of the fluid structure on the binding potential: Comparing liquid drop profiles from density functional theory with results from mesoscopic theory, *J. Chem. Phys.* **146**, 064705 (2017).
- [54] M. Elbaum and M. Schick, Application of the Theory of Dispersion Forces to the Surface Melting of Ice, *Phys. Rev. Lett.* **66**, 1713 (1991).
- [55] K. Binder, Finite size analysis of ising model block distribution functions, *Z. Phys. B* **43**, 119 (1981).
- [56] D. P. Landau and K. Binder, *A Guide to Monte Carlo Simulations in Statistical Physics* (Cambridge University Press, Cambridge, England, 2000).